Developing Improved Scaffolds for Fracture Healing: Macroporous Chitosan-Agarose-Gelatin Scaffolds Promote Cell Infiltration and are Significantly Tougher than Chitosan-Gelatin Cryogels

Leyi Chen[1,2], Yuseon Kim[1,4,5], Katherine R. Hixon[6], Nicole R. Gould[1], Andre F. Coello Hernandez[1,3], Matthew J. Silva[1,2,3]
Department of [1]Orthopedic Surgery, [2]Mechanical Engineering, [3]Biomedical Engineering, Washington University in St. Louis, St. Louis, MO
[4]Shriners Hospitals for Children—Saint Louis, St. Louis, MO 63110, USA
[5]Center of Regenerative Medicine, Washington University School of Medicine, St. Louis, MO
[6]Thayer School of Engineering, Dartmouth College, Hanover, NH

INTRODUCTION: Fracture nonunion occurs in 5-10% of patients. Surgical treatment of nonunion may require the use of bone graft, but it is an intensive surgery and has the potential to cause infection and donor site morbidity. Tissue engineering scaffolds are a promising alternative to bone graft because they can be made with tunable properties. Cryogels, which go through a freezing process during fabrication, can obtain enhanced porosity and strength as compared to hydrogels. In our lab, we previously induced osteogenesis at the femoral fracture site in the Col1-tk atrophic nonunion model using chitosan-gelatin (CG) scaffold-mediated delivery of BMP-2 by adipose-derived stem cells.[1] However, in that study, the sheet scaffolds tended to unwrap from the femur fracture site after the implantation. In addition, the thick layer and relatively small pore size of the scaffold may have hindered the cellular and vascular infiltration of the scaffold, as well as impaired integration of the scaffold bone with the native callus at the bone surface. CG cryogels were also relatively fragile and were challenging to keep intact during surgically implant. Herein, we used 3D printed molds to fabricate novel tube-shaped chitosan-agarose-gelatin (CAG) scaffolds to better conform to the geometry of the a long-bone (femoral) fractures site. We hypothesize that the addition of agarose and modifications to the fabrication process will result in increased pore size and improved physical properties in a way that will enhance cell infiltration. In future studies, we will use improved CAG scaffolds to deliver BMP-2 lentivirus (BMP2-LV) to have controllable and localized production of BMP-2 at the nonunion fracture site.

METHODS: To make tube-shaped scaffolds for future implantation around long-bones in mice, we created custom 3D printed molds (Fig.1) to fabricate scaffolds with the desired and consistent wall thickness of 0.5mm. For CG scaffolds, 80mg of chitosan and 320mg of gelatin were mixed in 8 ml of 1% acetic acid solution. 2ml of 1% glutaraldehyde was added to the mixture to initiate polymerization. The mixture was then decanted five times and poured into 3d-printed molds, followed by freezing at -20°C for 18h in methanol bath (condition I). Scaffolds were placed in -80°C for at least 1h before being lyophilized overnight. CAG scaffolds were fabricated in a similar way, except that the amount of chitosan, agarose and gelatin were 100mg, 300mg and 100mg, respectively. We controlled freezing rate of fabricating CAG scaffolds in three different ways, including frozen in methanol bath (cond. I), in air (cond. II), and in air with a sponge thermal isolator (cond. III). Microstructure of scaffolds was imaged using μCT 50 (Scanco). Pore diameter and porosity were quantified using trabecular separation (Tb. Sp) and bone volume fraction (BV/TV), respectively. Tensile test was performed on ElectroForce 3200 Mechanical Testing System (TA Instruments). Scaffolds for tensile test were trimmed into 20mmx3mm rectangular shape. All scaffolds were rehydrated before each test. Scaffolds were implanted subcutaneously in mice to evaluate biocompatibility and *in vivo* cell infiltration. Scaffolds for implantation were trimmed into 3mmx5mm rectangular shape. Cell infiltration was tested using confocal microscopy (Leica) after 7d subcutaneous implantation. Scaffolds were fixed and cryosectioned to a thickness of 100μm. A One-way ANOVA was used for microstructure and an unpaired t-test was used for mechanical properties. All *in vivo* procedures mentioned here were approved by institutional IACUC.

RESULTS: Determined by micro-CT, pore size and porosity of CAG scaffolds, independent of fabrication condition, is significantly larger and higher than CG scaffolds (Fig. 2A&B). The pore size of CAG and CG scaffolds, both fabricated with cond.I, is 40μm and 30μm, respectively (Fig. 2A), while the porosity of CAG cond.I and CG cond.I is 76% and 82%, respectively (Fig. 2B). The largest pore size was obtained when CAG scaffolds were fabricated via condition III, which can reach 75μm average pore diameter and 87.5% porosity (Fig. 2A&B). Tensile testing revealed that the post-yield-toughness of CAG scaffolds can reach 3kJ/m^3, which is significantly higher than CG scaffolds, which is only 0.01kJ/m^3 (Fig. 2C). In addition, the ultimate strain of CAG scaffolds can reach 30%, which is marginally higher than CG scaffolds, which is 25% (Fig. 2D). We also validated that both CG and CAG scaffolds allow cell infiltration and adhesion via confocal microscopy (Fig. 3). However, we found that cells are more restricted to the edge of CG scaffolds, as compared to CAG scaffolds where cells are able to infiltrate throughout the thickness of the scaffold (Fig. 3). Specifically, cells are most evenly distributed in CAG cond.II (Fig. 3B). We also directly coated scaffolds with GFP-lentivirus (GFP-LV), and, after subcutaneous implantation, we observed transduced, GFP-expressing cells in CG and CAG scaffolds.

DISCUSSION: Taken together, these results show that adjusting freezing rate is an efficient way to control the porosity and pore size of cryogel scaffolds. Both CG and CAG scaffolds have porosity over 75%, but CAG scaffolds have much larger pore size than CG scaffolds, which is more ideal for cell infiltration and angiogenesis. Tensile testing validates that CG scaffolds are more brittle than CAG scaffolds with negligible post-yield-toughness, which makes CAG scaffolds more suitable for surgical manipulation. Both CG and CAG scaffolds can allow cell infiltration and adhesion *in vivo*, but cells show a great tendency to get stuck at the edge of CG scaffolds, perhaps due to small pore size. As a result, cells in CAG scaffolds should be more likely to get transduced by BMP2-LV. Overall, CAG scaffolds show more prominent microstructure, cell infiltration and mechanical properties than CG scaffolds, which may serve as a better vehicle for BMP2-LV delivery for *in vivo* implantation.

SIGNIFICANCE/CLINICAL RELAVENCE: Current treatments for atrophic nonunion fracture is expensive, time-consuming, and highly invasive with a fairly low success rate. Highly controllable and localized delivery of BMP-2 using non-toxic, degradable, and porous scaffolds can serve as a promising and efficient substitute to the existing treatments to rescue atrophic nonunion fracture.

REFERENCES:

1. Hixon KR, Katz DB, McKenzie JA, Miller AN, Guilak F, Silva MJ. Cryogel Scaffold-Mediated Delivery of Adipose-Derived Stem Cells Promotes Healing in Murine Model of Atrophic Non-Union. Front Bioeng Biotechnol. 2022 May 5;10:851904.

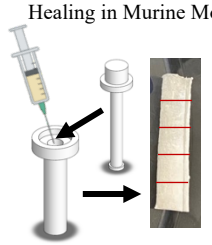

Figure 1: Illustration of a 3D printed mold used for scaffolds fabrication

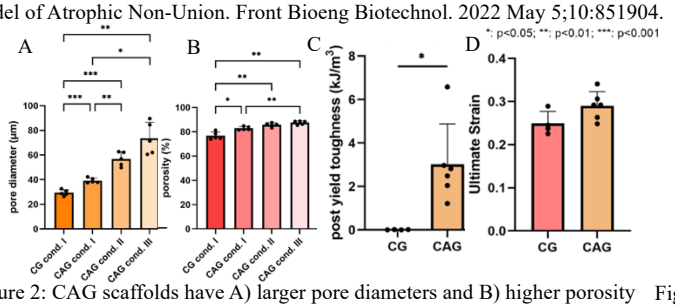

Figure 2: CAG scaffolds have A) larger pore diameters and B) higher porosity than CG scaffolds independent of freezing rate. CAG scaffolds are significantly tougher than CG scaffolds with C) higher PYT and D) ultimate strain

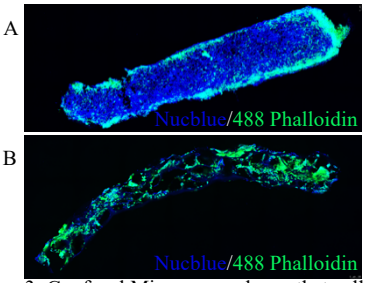

Figure 3: Confocal Microscopy shows that cells are more easily to infiltrate into CAG scaffolds. Gelatin has autofluorescence in blue. (Scale Bar: 100 μm).